Covariance Analysis of Maximum Likelihood Attitude Estimation[1]

Joanna C. Hinks[2] and John L. Crassidis[3]

ABSTRACT

An attitude determination covariance measurement model for unit vector sensors with a wide field-of-view is analyzed and compared to the classic QUEST covariance model. The wide field-of-view model has been previously proposed as a more realistic alternative for sensors where measurement accuracy depends on angular distance from the boresight axis. Both QUEST and the wide field-of-view models are evaluated relative to a measurement model that uses the two-dimensional sensor focal plane measurements directly, rather than first converting them to unit vectors. The Cramér-Rao lower bound is derived for attitude determination based on such direct sensor measurements, and the wide field-of-view measurement model is shown to achieve this Cramér-Rao lower bound. Numerical simulations confirm that an extended Kalman filter based on the wide field-of-view model outperforms a filter based on the QUEST model, and also that the wide field-of-view 3σ bounds are effectively identical to those of a filter based on the direct two-dimensional sensor measurements.

INTRODUCTION

One of the requirements of most spacecraft missions is attitude determination. In this process, some combination of sensor measurements is used to determine the orientation of a spacecraft with respect to some chosen reference frame. Some attitude determination methods process a batch of measurements that apply at a specific instant in time. In particular, many strategies have been developed to find the optimal attitude by minimizing the Wahba problem cost function [1]. Other techniques estimate the attitude history of a dynamically-rotating spacecraft by applying an extended Kalman filter (EKF) or other filtering algorithms [2, 3, 4, 5]. For a survey of approaches to attitude determination, see Ref. [6].

Common sensors for attitude determination include three-axis magnetometers, Sun sensors, Earth-horizon sensors, star trackers and onboard GPS receivers [7]. In the context of filtering, these are often combined with gyroscopic rate measurements. Attitude determination strategies, both static and dynamic, require accurate mathematical models that relate each distinct type of measurement to the spacecraft attitude. Measurement models have two components. First,

[1]This paper is dedicated to the memory of Dr. Malcolm D. Shuster and the Acme Spacecraft Company.

[2]Postdoctoral Assistant, Department of Mechanical & Aerospace Engineering, University at Buffalo, State University of New York, Amherst, NY, 14260-4400. Email: jchinks@buffalo.edu.

[3]Professor, Department of Mechanical & Aerospace Engineering, University at Buffalo, State University of New York, Amherst, NY, 14260-4400. Email: johnc@buffalo.edu.

they require an equation that relates the measured quantity to the state of interest (in this case, some parameterization of attitude). Second, there must be a statistical description of the errors in the measurements.

Attitude determination sensors most frequently measure line-of-sight (LOS) directions to some point of reference in a frame of reference that moves with the spacecraft body. For instance, a sensor may observe the direction to the Sun, or the direction of the local magnetic field lines, or the directions to known stars. Two such direction measurements at a given instant serve to fix the spacecraft orientation relative to the reference frame (which is typically inertial). LOS directions are usually reported as three-dimensional vectors having unit length. The unit-length constraint means that the measurement actually contains only two pieces of scalar information in its three elements, and this can cause problems for attitude determination algorithms. The simplest measurement models contain additive random noise that is distributed as a Gaussian with some mean and covariance. In the case of unit vectors, however, the errors must be constrained to those that, when added to the true unit vector, change its direction but not its length. In other words, the uncertainty lies on the surface of the unit sphere. A consequence of this constraint is that the associated 3×3 measurement error covariance matrices are singular, with a zero eigenvalue corresponding to an eigenvector aligned with the measurement. The traditional Kalman filtering equations require inversion of the measurement covariance, so special modifications are necessary.

One of the most widely used models for LOS measurements is Shuster's QUaternion ESTimator (QUEST) measurement model [8]. This model recognizes that most of the measurement uncertainty is concentrated in a region very close to the true direction, where the surface of the unit sphere can be well-approximated by a tangent plane. The resulting measurement error covariance matrix is a scalar multiple of the projection matrix that projects arbitrary vectors onto a plane orthogonal to the measurement vector. While the assumptions of QUEST are reasonable for arbitrary unit vectors, this model does not account for the physical characteristics of the sensors that measured those vectors.

Missions that require precise attitude knowledge and/or control most frequently use star trackers. Star trackers based on charge-coupled devices (CCD) measure the angle from the camera boresight to a star in two mutually orthogonal planes, and can achieve accuracies on the order of 10 to 20 arcsec [9]. For star trackers with a very narrow field-of-view (FOV), the QUEST measurement model closely approximates the true uncertainty distribution. Historically, wide-FOV attitude sensors have been less accurate, so that differences between the QUEST covariance and the true measurement covariance were relatively insignificant [5]. Recent technological advances have resulted in more accurate wide field-of-view sensors. In particular, the vision-based navigation (VISNAV) system [10] employs a Position Sensing Diode (PSD) in the focal plane of a wide-angle lens to achieve a 100 degree FOV. These technological improvements motivated a new wide-FOV measurement model [11], which takes into account the increased sensor noise far from the sensor boresight. Reference [11] develops a new measurement model, presents an EKF framework based on this model, and shows improved performance over the QUEST model in numerical simulations.

The QUEST measurement model has been extensively studied in the past decades. Shuster explored the validity

of its assumptions [12], showed how it could be implemented in a Kalman filter [4, 5], and clarified its theoretical connections to Wahba's problem and to maximum likelihood estimation [12, 13]. Although the wide-FOV model seems intuitively reasonable and has been shown to outperform QUEST in specific simulations, it has not been subjected to the same rigorous analysis. The present paper seeks to bridge that gap. Both QUEST and the new wide-FOV measurement model are examined in the context of the star tracker focal plane model. The Fisher information matrix (FIM) for the inherently two-dimensional star tracker measurements is calculated, and this matrix is compared to the corresponding quantities for QUEST and the wide-FOV model. Additional derivations highlight some interesting matrix properties. Note that although QUEST and the wide-FOV model are the focus of this paper, other LOS vector measurement models are possible. In particular, the Multiplicative Measurement Model [14] employs multiplicative rather than additive measurement noise so as to enforce the unit-length constraint by construction. The development of a Kalman filter framework for attitude determination with multiplicative measurement noise is beyond the scope of the present work.

The remainder of this paper is organized as follows. First, the details of the QUEST measurement model and the wide-FOV measurement model, as presented in Ref. [11], are summarized to provide necessary background information and terminology. Next, the measurement sensitivity matrix for the 2D star tracker focal plane measurements is developed, and the expression for the corresponding Fisher information matrix is given. The wide-FOV measurement model is then analyzed and compared to the 2D focal plane model and the theoretical Cramér-Rao lower bound (CRLB). The QUEST measurement model is compared to this same bound, and some properties of the estimation error covariance matrices for each measurement model are derived. Finally, the numerical simulations of Ref. [11] are repeated alongside an EKF based on 2D star tracker focal plane measurements to illustrate the paper's theoretical results.

BACKGROUND

This section provides necessary background information and establishes notation related to the QUEST and wide-FOV measurement models. Many of the equations are from Ref. [11], along with some more detailed explanations.

Star trackers form measurements according to a set of *collinearity equations*, which are standard in many photogrammetry applications [15]. Assuming that the camera boresight is aligned with the z-axis, these are given by

$$\alpha_i = -f\frac{A_{11}\left(X_i - x\right) + A_{12}\left(Y_i - y\right) + A_{13}\left(Z_i - z\right)}{A_{31}\left(X_i - x\right) + A_{32}\left(Y_i - y\right) + A_{33}\left(Z_i - z\right)}, \qquad i = 1, 2, \ldots, N \tag{1a}$$

$$\beta_i = -f\frac{A_{21}\left(X_i - x\right) + A_{22}\left(Y_i - y\right) + A_{23}\left(Z_i - z\right)}{A_{31}\left(X_i - x\right) + A_{32}\left(Y_i - y\right) + A_{33}\left(Z_i - z\right)}, \qquad i = 1, 2, \ldots, N \tag{1b}$$

The observation vector that is directly measured by the tracker is therefore

$$\boldsymbol{\gamma}_i \equiv \begin{bmatrix} \alpha_i \\ \beta_i \end{bmatrix} \tag{2}$$

and the corresponding measurement equation with noise is

$$\tilde{\boldsymbol{\gamma}}_i = \boldsymbol{\gamma}_i + \mathbf{w}_i \tag{3}$$

The zero-mean Gaussian noise process $\mathbf{w}_i$ is assumed to have the covariance:

$$R_i^{\mathrm{FOCAL}} = \frac{\sigma^2}{1 + d\left(\alpha_i^2 + \beta_i^2\right)} \begin{bmatrix} \left(1 + d\alpha_i^2\right)^2 & \left(d\alpha_i\beta_i\right)^2 \\ \left(d\alpha_i\beta_i\right)^2 & \left(1 + d\beta_i^2\right)^2 \end{bmatrix} \tag{4}$$

where d is on the order of one (and often simply set to one) and σ is assumed to be known [5].

In unit vector form, the observations are

$$\mathbf{b}_i = A\mathbf{r}_i, \qquad i = 1, 2, \ldots, N \tag{5}$$

where

$$\mathbf{b}_i \equiv \frac{1}{\sqrt{1 + \alpha_i^2 + \beta_i^2}} \begin{bmatrix} -\alpha_i \\ -\beta_i \\ 1 \end{bmatrix} \tag{6a}$$

$$\mathbf{r}_i \equiv \frac{1}{\sqrt{\left(X_i - x\right)^2 + \left(Y_i - y\right)^2 + \left(Z_i - z\right)^2}} \begin{bmatrix} X_i - x \\ Y_i - y \\ Z_i - z \end{bmatrix} \tag{6b}$$

The measurement equation for the unit vector (as used in the QUEST algorithm [8]) is

$$\tilde{\mathbf{b}}_i = A\mathbf{r}_i + \boldsymbol{\upsilon}_i, \qquad \boldsymbol{\upsilon}_i^{\mathrm{T}}\mathbf{b}_i = 0 \tag{7}$$

where the statistics of the noise $\boldsymbol{\upsilon}_i$ are given by

$$\mathrm{E}\{\boldsymbol{\upsilon}_i\} = \mathbf{0} \tag{8a}$$

$$R_i^{\mathrm{QUEST}} \equiv \mathrm{E}\left\{\boldsymbol{\upsilon}_i\boldsymbol{\upsilon}_i^{\mathrm{T}}\right\} = \sigma^2\left(I_{3\times 3} - \mathbf{b}_i\mathbf{b}_i^{\mathrm{T}}\right) \tag{8b}$$

The QUEST measurement model makes the generally reasonable assumption that the uncertainty in the line-of-sight

(LOS) unit vector measurement lies in the tangent plane to the unit sphere at the point where it intersects the measurement. This assumption becomes less valid for sensors with a wide field of view (FOV) and LOS vectors far from the boresight direction.

To derive the wide field-of-view covariance model, the 2×2 covariance R_i^{FOCAL} from equation (4) is transformed to a rank-deficient 3×3 covariance matrix (R_i^{wFOV}) via the Jacobian:

$$J_i \equiv \frac{\partial \mathbf{b}_i}{\partial \boldsymbol{\gamma}_i} = \frac{1}{\sqrt{1+\alpha_i^2+\beta_i^2}} \begin{bmatrix} -1 & 0 \\ 0 & -1 \\ 0 & 0 \end{bmatrix} - \frac{1}{1+\alpha_i^2+\beta_i^2} \mathbf{b}_i \begin{bmatrix} \alpha_i & \beta_i \end{bmatrix} \tag{9}$$

With this J_i, the new covariance is given by

$$R_i^{\mathrm{wFOV}} = J_i R_i^{\mathrm{FOCAL}} J_i^{\mathrm{T}} \tag{10}$$

Note that Ref. [11] calls this covariance R_i^{NEW}. As this covariance is no longer a "new" result, the notation R_i^{wFOV} is adopted.

The QUEST covariance can also be written in terms of the Jacobian [5, 16]:

$$R_i^{\mathrm{QUEST}} = J_i \mathbb{R}_i^{\mathrm{FOCAL}} J_i^{\mathrm{T}} \tag{11}$$

where

$$\mathbb{R}_i^{\mathrm{FOCAL}} \equiv \sigma^2 \left(1+\alpha_i^2+\beta_i^2\right) \begin{bmatrix} 1+\alpha_i^2 & \alpha_i\beta_i \\ \alpha_i\beta_i & 1+\beta_i^2 \end{bmatrix} \tag{12}$$

This paper deals extensively with matrix-valued inequalities. The standard convention is used: Given two matrices A and B, one writes $A \geq B$ or $A - B \geq 0$ if the difference matrix $A - B$ is positive semidefinite. It has been proven in Ref. [11] that $R_i^{\mathrm{QUEST}} \geq R_i^{\mathrm{wFOV}}$ for all d in the range $0 \leq d \leq 1$. In order to obtain this result, that source also proves that $\mathbb{R}_i^{\mathrm{FOCAL}} \geq R_i^{\mathrm{FOCAL}}$. It also employs the fact that the eigenvalues of the matrix $\mathbb{R}_i^{\mathrm{FOCAL}}$ are $\sigma^2\left(1+\alpha_i^2+\beta_i^2\right)$ and $\sigma^2\left(1+\alpha_i^2+\beta_i^2\right)^2$. These results will be required in what follows.

Shuster demonstrated [12, 13] that the Wahba problem [1], with suitable weights, is equivalent to a maximum likelihood estimation problem for attitude. Specifically, the Wahba problem assumes LOS unit-vector measurements $\mathbf{b}_i$, as in equation (5), and seeks the attitude matrix A that minimizes the cost

$$L(A) = \frac{1}{2} \sum_{i=1}^{N} a_i \left|\mathbf{b}_i - A\mathbf{r}_i\right|^2 \tag{13}$$

When the weights are chosen as $a_i = 1/\sigma_i^2$, this cost function is minimized by the same attitude matrix A that maximizes the likelihood function:

$$p_{\mathbf{b}_1,\mathbf{b}_2,\ldots,\mathbf{b}_N}\left(\tilde{\mathbf{b}}_1,\tilde{\mathbf{b}}_2,\ldots,\tilde{\mathbf{b}}_N|A\right) = \prod_{i=1}^{N} C_i \exp\left\{-\frac{1}{2\sigma_i^2}\left|\tilde{\mathbf{b}}_i - A\mathbf{r}_i\right|^2\right\} \tag{14}$$

where the scalar constant C_i is computed so as to properly normalize the function. Shuster further showed [12, 13] that the inverse of the Fisher information matrix (FIM) [17] for that problem is given by

$$F^{-1}_{\boldsymbol{\delta\mathbf{a}}\boldsymbol{\delta\mathbf{a}}} = \left[\sum_{i=1}^{N}\frac{1}{\sigma_i^2}\left(I_{3\times 3} - \mathbf{b}_i\mathbf{b}_i^{\mathrm{T}}\right)\right]^{-1} = \left[\sum_{i=1}^{N}\frac{1}{\sigma_i^4}R_i^{\mathrm{QUEST}}\right]^{-1} = P^{\mathrm{QUEST}} \tag{15}$$

In other words, the inverse of the Fisher information matrix for the Wahba problem yields P^{QUEST}, which has been shown to be the attitude error covariance matrix for the QUEST algorithm [8]. Shuster's results require, however, that the sensor measurements behave according to the QUEST measurement model of equation (8). The QUEST measurement model assumes a reasonable distribution for the errors in the LOS vectors, and this distribution dictates a corresponding focal plane covariance that has no basis in the physics of the actual sensor. The following section starts from the sensor model and works up to derive the attitude estimation error covariance directly. Note also that in the following sections, the measurement error standard deviation σ has been assumed to be measurement-independent when it appears in the expressions for R_i^{FOCAL}, $\mathbb{R}_i^{\mathrm{FOCAL}}$, and so forth.

COVARIANCE DIRECTLY FROM 2-D STAR OBSERVATIONS

This section works with the two-dimensional sensor measurement model, and derives the relationship between attitude estimate errors and sensor errors. Some of the following results are presented in Ref. [5] without a thorough derivation. Furthermore, that source employed the sensor model only for its truth model and not for filtering, and no rigorous analysis of the sensor model covariance properties was performed. An alternative, equivalent derivation is also available in Ref. [13].

The following assumptions have been made in this section's derivations:

1. The observation errors are small relative to the observations themselves, i.e., the signal-to-noise ratio is large enough to maintain Gaussian statistics throughout the derivations.

2. The boresight vector is aligned with the camera-frame z-axis.

First, it is possible to write the observations α_i and β_i as nonlinear functions of the true attitude matrix A. Let $\mathbf{x} = [1 \quad 0 \quad 0]^{\mathrm{T}}$, $\mathbf{y} = [0 \quad 1 \quad 0]^{\mathrm{T}}$, and $\mathbf{z} = [0 \quad 0 \quad 1]^{\mathrm{T}}$. Then equation (1) can be rewritten as:

$$\alpha_i = -\frac{\mathbf{x}^{\mathrm{T}}A\mathbf{r}_i}{\mathbf{z}^{\mathrm{T}}A\mathbf{r}_i} \tag{16a}$$

$$\beta_i = -\frac{\mathbf{y}^{\mathrm{T}} A \mathbf{r}_i}{\mathbf{z}^{\mathrm{T}} A \mathbf{r}_i} \tag{16b}$$

As is common for nonlinear measurement functions, a linearization is performed about the true attitude. Such a procedure expresses the measurement residual (the difference between the true measurement vector and the one predicted based on the attitude estimate) as a linear function of the error in the attitude estimate. Let $\boldsymbol{\delta}\mathbf{a}$ be a random zero-mean Gaussian vector of small-angle errors in the attitude estimate $\widehat{A}$, such that:

$$\widehat{A} \approx \left(I_{3\times 3} - [\boldsymbol{\delta}\mathbf{a}\times]\right) A, \qquad A \approx \left(I_{3\times 3} + [\boldsymbol{\delta}\mathbf{a}\times]\right) \widehat{A} \tag{17}$$

where the $[\boldsymbol{\delta}\mathbf{a}\times]$ denotes the standard cross-product matrix corresponding to the vector $\boldsymbol{\delta}\mathbf{a}$.

The following derivations are specific to the x-axis observation α_i. It is understood that equivalent calculations can be carried out for the y-axis observation β_i in the same fashion.

Let $\hat{\alpha}_i$ be the value of α_i that would be expected for a given reference vector $\mathbf{r}_i$ and the attitude matrix estimate $\widehat{A}$. It can be written in terms of the true attitude matrix A and the error vector $\boldsymbol{\delta}\mathbf{a}$ as:

$$\hat{\alpha}_i \equiv -\frac{\mathbf{x}^{\mathrm{T}} \widehat{A} \mathbf{r}_i}{\mathbf{z}^{\mathrm{T}} \widehat{A} \mathbf{r}_i} = \frac{-\mathbf{x}^{\mathrm{T}} A \mathbf{r}_i - \mathbf{x}^{\mathrm{T}} [A\mathbf{r}_i\times]\, \boldsymbol{\delta}\mathbf{a}}{\mathbf{z}^{\mathrm{T}} A \mathbf{r}_i + \mathbf{z}^{\mathrm{T}} [A\mathbf{r}_i\times]\, \boldsymbol{\delta}\mathbf{a}} \tag{18}$$

Now form the difference $h_\alpha\left(\boldsymbol{\delta}\mathbf{a}\right) = \hat{\alpha}_i - \alpha_i$.

$$\begin{aligned} h_\alpha\left(\boldsymbol{\delta}\mathbf{a}\right) &= \hat{\alpha}_i - \alpha_i \\ &= -\frac{\left(-\mathbf{x}^{\mathrm{T}} \widehat{A} \mathbf{r}_i - \mathbf{x}^{\mathrm{T}} [A\mathbf{r}_i\times]\, \boldsymbol{\delta}\mathbf{a}\right)\left(\mathbf{z}^{\mathrm{T}} A \mathbf{r}_i\right)}{\left(\mathbf{z}^{\mathrm{T}} A \mathbf{r}_i + \mathbf{z}^{\mathrm{T}} [A\mathbf{r}_i\times]\, \boldsymbol{\delta}\mathbf{a}\right)\left(\mathbf{z}^{\mathrm{T}} A \mathbf{r}_i\right)} - \frac{\left(\mathbf{x}^{\mathrm{T}} A \mathbf{r}_i\right)\left(\mathbf{z}^{\mathrm{T}} A \mathbf{r}_i + \mathbf{z}^{\mathrm{T}} [A\mathbf{r}_i\times]\, \boldsymbol{\delta}\mathbf{a}\right)}{\left(\mathbf{z}^{\mathrm{T}} A \mathbf{r}_i\right)\left(\mathbf{z}^{\mathrm{T}} A \mathbf{r}_i + \mathbf{z}^{\mathrm{T}} [A\mathbf{r}_i\times]\, \boldsymbol{\delta}\mathbf{a}\right)} \\ &= \frac{-\left(\mathbf{x}^{\mathrm{T}} A \mathbf{r}_i\right)\left(\mathbf{z}^{\mathrm{T}} A \mathbf{r}_i\right) - \left(\mathbf{x}^{\mathrm{T}} [A\mathbf{r}_i\times]\, \boldsymbol{\delta}\mathbf{a}\right)\left(\mathbf{z}^{\mathrm{T}} A \mathbf{r}_i\right) + \left(\mathbf{x}^{\mathrm{T}} A \mathbf{r}_i\right)\left(\mathbf{z}^{\mathrm{T}} A \mathbf{r}_i\right) + \left(\mathbf{x}^{\mathrm{T}} A \mathbf{r}_i\right)\left(\mathbf{z}^{\mathrm{T}} [A\mathbf{r}_i\times]\, \boldsymbol{\delta}\mathbf{a}\right)}{\left(\mathbf{z}^{\mathrm{T}} A \mathbf{r}_i + \mathbf{z}^{\mathrm{T}} [A\mathbf{r}_i\times]\, \boldsymbol{\delta}\mathbf{a}\right)\left(\mathbf{z}^{\mathrm{T}} A \mathbf{r}_i\right)} \\ &= \frac{-\mathbf{x}^{\mathrm{T}} [A\mathbf{r}_i\times]\, \boldsymbol{\delta}\mathbf{a} - \alpha_i \mathbf{z}^{\mathrm{T}} [A\mathbf{r}_i\times]\, \boldsymbol{\delta}\mathbf{a}}{\mathbf{z}^{\mathrm{T}} A \mathbf{r}_i + \mathbf{z}^{\mathrm{T}} [A\mathbf{r}_i\times]\, \boldsymbol{\delta}\mathbf{a}} \end{aligned} \tag{19}$$

By the same process, one can obtain the expression for the difference $h_\beta\left(\boldsymbol{\delta}\mathbf{a}\right) = \hat{\beta}_i - \beta_i$:

$$h_\beta\left(\boldsymbol{\delta}\mathbf{a}\right) = \hat{\beta}_i - \beta_i = \frac{-\mathbf{y}^{\mathrm{T}} [A\mathbf{r}_i\times]\, \boldsymbol{\delta}\mathbf{a} - \beta_i \mathbf{z}^{\mathrm{T}} [A\mathbf{r}_i\times]\, \boldsymbol{\delta}\mathbf{a}}{\mathbf{z}^{\mathrm{T}} A \mathbf{r}_i + \mathbf{z}^{\mathrm{T}} [A\mathbf{r}_i\times]\, \boldsymbol{\delta}\mathbf{a}} \tag{20}$$

Equations (19) and (20) resemble the nonlinear equation $\Delta\mathbf{y} = h\left(\Delta\mathbf{x}\right)$. To compute the standard nonlinear least-squares correction for the current estimate of $\Delta\mathbf{x}$, one linearizes this equation about that current estimate to obtain an equation of the form $\Delta\mathbf{y} \approx H\Delta\mathbf{x}$. The covariance of $\Delta\mathbf{x}$ in this equation is given by $\left(H^{\mathrm{T}} R^{-1} H\right)^{-1}$, where R is the covariance associated with the observation $\Delta\mathbf{y}$.

In this specific case, the observations $\Delta\mathbf{y}$ are α_i and β_i, and $\boldsymbol{\delta}\mathbf{a}$ plays the role of $\Delta\mathbf{x}$. The linearization can be

computed by expanding Eqs. (19) and (20) in a Taylor series about the small attitude error vector $\boldsymbol{\delta}\mathbf{a} \approx \mathbf{0}$, and neglecting higher order terms:

$$\begin{bmatrix} \hat{\alpha}_i - \alpha_i \\ \hat{\alpha}_i - \alpha_i \end{bmatrix} \approx \left(\begin{bmatrix} h_\alpha(\boldsymbol{\delta}\mathbf{a}) \\ h_\alpha(\boldsymbol{\delta}\mathbf{a}) \end{bmatrix}_{\boldsymbol{\delta}\mathbf{a}=\mathbf{0}} \right) + \left(\frac{\partial}{\partial \boldsymbol{\delta}\mathbf{a}} \begin{bmatrix} h_\alpha(\boldsymbol{\delta}\mathbf{a}) \\ h_\alpha(\boldsymbol{\delta}\mathbf{a}) \end{bmatrix}_{\boldsymbol{\delta}\mathbf{a}=\mathbf{0}} \right) \boldsymbol{\delta}\mathbf{a} + \mathcal{O}\left(\boldsymbol{\delta}\mathbf{a}^2\right) \tag{21}$$

The first term in the Taylor series is zero when $\boldsymbol{\delta}\mathbf{a} = \mathbf{0}$. The matrix H arises in the second term as the Jacobian for the vector $[h_\alpha,\ h_\beta]^{\mathrm{T}}$, evaluated at $\boldsymbol{\delta}\mathbf{a} = \mathbf{0}$. After simplification, the result is given by:

$$H_i = \frac{\partial}{\partial \boldsymbol{\delta}\mathbf{a}} \begin{bmatrix} h_\alpha(\boldsymbol{\delta}\mathbf{a}) \\ h_\beta(\boldsymbol{\delta}\mathbf{a}) \end{bmatrix}_{\boldsymbol{\delta}\mathbf{a}=\mathbf{0}} = -\frac{1}{\mathbf{z}^{\mathrm{T}}\mathbf{b}_i} \begin{bmatrix} \mathbf{x}^{\mathrm{T}} + \alpha_i \mathbf{z}^{\mathrm{T}} \\ \mathbf{y}^{\mathrm{T}} + \beta_i \mathbf{z}^{\mathrm{T}} \end{bmatrix} [\mathbf{b}_i \times] = -\frac{1}{\mathbf{z}^{\mathrm{T}}\mathbf{b}_i} \begin{bmatrix} \mathbf{x}^{\mathrm{T}} \\ \mathbf{y}^{\mathrm{T}} \end{bmatrix} \left(I_{3\times 3} - \frac{\mathbf{b}_i \mathbf{z}^{\mathrm{T}}}{\mathbf{z}^{\mathrm{T}}\mathbf{b}_i} \right) [\mathbf{b}_i \times] \tag{22}$$

where $\mathbf{b}_i = A\mathbf{r}_i$ as per equation (5). The matrix H_i has a simple geometric interpretation, which is most clearly expressed in the rightmost part of equation (22). Recall that H_i multiplies the incremental attitude error vector $\boldsymbol{\delta}\mathbf{a}$ to produce the focal plane measurement errors $\hat{\alpha}_i - \alpha_i$ and $\hat{\beta}_i - \beta_i$. The cross product matrix $[\mathbf{b}_i \times]$ extracts the component of $\boldsymbol{\delta}\mathbf{a}$ orthogonal to the measurement $\mathbf{b}_i$. Attitude errors corresponding to rotations around $\mathbf{b}_i$ do not cause focal plane measurement errors. Next, the matrix difference in the rightmost part of equation (22) is an oblique projection matrix, which projects the remaining attitude error along the LOS measurement vector direction and onto the focal plane. The final components of H_i separate the α_i and β_i parts of the focal plane measurement error and scale the error appropriately.

As noted above, equation (20) resembles a linearized least-squares problem for the unknown state $\boldsymbol{\delta}\mathbf{a}$, with measurement $\hat{\beta}_i - \beta_i$, measurement sensitivity matrix H_i, and measurement covariance R_i^{FOCAL}. The least-squares solution for $\boldsymbol{\delta}\mathbf{a}$ has estimation error covariance $\left[H_i^{\mathrm{T}} \left(R_i^{\mathrm{FOCAL}}\right)^{-1} H_i\right]^{-1}$. Because this is a least-squares problem with Gaussian noise, the one-measurement Fisher information matrix [17] is the inverse of the estimation error covariance: $H_i^{\mathrm{T}} \left(R_i^{\mathrm{FOCAL}}\right)^{-1} H_i$. The corresponding Cramér-Rao lower bound (CRLB) for N measurements is given by

$$P^{\mathrm{DIRECT}} = \left[\sum_{i=1}^{N} H_i^{\mathrm{T}} \left(R_i^{\mathrm{FOCAL}}\right)^{-1} H_i \right]^{-1} \tag{23}$$

THE WIDE-FOV COVARIANCE MODEL AND THE CRAMÉR-RAO LOWER BOUND

It is possible to derive a simple expression for the relationship between the wide-FOV covariance R_i^{wFOV} and the newly-derived FIM. This relationship further allows one to compare the wide-FOV estimation error covariance, P^{wFOV}, to the CRLB of equation (23). These derivations hold for the range $0 \leq d \leq 1$, where d is the parameter from R_i^{FOCAL}.

First, substitute equation (6a) into equation (22) to obtain an expression for the matrix H_i in terms of the α_i and β_i

observations:

$$H_i = \begin{bmatrix} -\alpha_i\beta_i & \left(1+\alpha_i^2\right) & \beta_i \\ -\left(1+\beta_i^2\right) & \alpha_i\beta_i & -\alpha_i \end{bmatrix} \tag{24}$$

Using this expression for H_i, it can be shown that the Jacobian matrix J_i from equation (9) can be written as

$$J_i = \frac{1}{\left(1+\alpha_i^2+\beta_i^2\right)^{3/2}} H_i^{\mathrm{T}} \begin{bmatrix} 0 & -1 \\ 1 & 0 \end{bmatrix} \tag{25}$$

The 2×2 matrix on the right in equation (25) has an interesting property: it can be used to transform any symmetric 2×2 matrix into the adjugate of that matrix. The transformation takes the form

$$\begin{bmatrix} 0 & -1 \\ 1 & 0 \end{bmatrix} \begin{bmatrix} a & b \\ b & c \end{bmatrix} \begin{bmatrix} 0 & -1 \\ 1 & 0 \end{bmatrix}^{\mathrm{T}} = \begin{bmatrix} c & -b \\ -b & a \end{bmatrix} = \mathrm{adj}\left(\begin{bmatrix} a & b \\ b & c \end{bmatrix} \right) \tag{26}$$

where "adj" represents the matrix adjugate operation. The adjugate of a matrix A is related to the matrix inverse by the scalar determinant: $\mathrm{adj}\left(A\right) = \det\left(A\right) A^{-1}$.

These properties can be exploited along with the new form of the Jacobian in equation (25) to write a new expression for the measurement covariance R_i^{wFOV}. Equation (10) becomes

$$\begin{aligned} R_i^{\mathrm{wFOV}} &= \frac{1}{\left(1+\alpha_i^2+\beta_i^2\right)^{3/2}} H_i^{\mathrm{T}} \begin{bmatrix} 0 & -1 \\ 1 & 0 \end{bmatrix} R_i^{\mathrm{FOCAL}} \begin{bmatrix} 0 & 1 \\ -1 & 0 \end{bmatrix} H_i \frac{1}{\left(1+\alpha_i^2+\beta_i^2\right)^{3/2}} \\ &= \frac{1}{\left(1+\alpha_i^2+\beta_i^2\right)^{3}} H_i^{\mathrm{T}} \det\left(R_i^{\mathrm{FOCAL}}\right) \left(R_i^{\mathrm{FOCAL}}\right)^{-1} H_i \end{aligned} \tag{27}$$

One can further simplify equation (27) by recalling that $\det\left(\mathbb{R}_i^{\mathrm{FOCAL}}\right) = \sigma^4 \left(1+\alpha_i^2+\beta_i^2\right)^3$ [11]. Equation (27) reduces to

$$\begin{aligned} R_i^{\mathrm{wFOV}} &= \frac{\sigma^4 \det\left(R_i^{\mathrm{FOCAL}}\right)}{\det\left(\mathbb{R}_i^{\mathrm{FOCAL}}\right)} H_i^{\mathrm{T}} \left(R_i^{\mathrm{FOCAL}}\right)^{-1} H_i \\ &= \sigma^4 \eta_i H_i^{\mathrm{T}} \left(R_i^{\mathrm{FOCAL}}\right)^{-1} H_i \end{aligned} \tag{28}$$

where the scalar function η_i is $\det\left[R_i^{\mathrm{FOCAL}} \left(\mathbb{R}_i^{\mathrm{FOCAL}}\right)^{-1}\right]$. The scalar η_i is a function of the variables d, α_i, and β_i, and can be written out explicitly as

$$\eta_i\left(\alpha_i, \beta_i, d\right) \equiv \frac{\left(1+d\alpha_i^2\right)\left(1+d\beta_i^2\right) + \left(d\alpha_i\beta_i\right)^2}{\left(1+\alpha_i^2+\beta_i^2\right)^3 \left[1+d\left(\alpha_i^2+\beta_i^2\right)\right]} \tag{29}$$

The thrust of equation (28) is that R_i^{wFOV} is just an observation-dependent scalar multiple of the single-observation

FIM.

Now examine the properties of the scalar function η_i more closely. It is straightforward to show that $0 < \eta_i \leq 1$ for all observations α_i and β_i and all d in the range from zero to one. To establish the lower bound on η_i, examine its numerator and denominator individually. For convenience, call them η_i^{num} and η_i^{den}, respectively. The first term in η_i^{num} is a product of two expressions that are greater than or equal to one, and the second term is a squared quantity, so neither can be negative. Therefore η_i^{num} is always non-negative. Likewise, η_i^{den} is a product of terms that are greater than or equal to one for all α_i, β_i, and $d \in (0, 1)$. As η_i^{den} is also non-negative, $\eta_i = \eta_i^{\text{num}}/\eta_i^{\text{den}} > 0$.

If η_i has an upper bound of 1, η_i^{num} is always less than or equal to η_i^{den}. This property can be verified by multiplying out the expressions for η_i^{num} and η_i^{den} and showing that the difference $\eta_i^{\text{num}} - \eta_i^{\text{den}} \leq 0$:

$$\begin{aligned}
\eta_i^{\text{num}} - \eta_i^{\text{den}} &= \left(1 + d\alpha_i^2\right)\left(1 + d\beta_i^2\right) + \left(d\alpha_i\beta_i\right)^2 - \left(1 + \alpha_i^2 + \beta_i^2\right)^3\left[1 + d\left(\alpha_i^2 + \beta_i^2\right)\right] \\
&= \left[1 + d\left(\alpha_i^2 + \beta_i^2\right)\right] + 2\left(d\alpha_i\beta_i\right)^2 - \left[1 + d\left(\alpha_i^2 + \beta_i^2\right)\right]\left(1 + 3\alpha_i^2 + 3\beta_i^2 + 6\alpha_i^2\beta_i^2 + \ldots\right) \\
&= 2\left(d\alpha_i\beta_i\right)^2 - \left[1 + d\left(\alpha_i^2 + \beta_i^2\right)\right]\left(3\alpha_i^2 + 3\beta_i^2 + 6\alpha_i^2\beta_i^2 + \ldots\right) \\
&= 2\left(d\alpha_i\beta_i\right)^2 - 2\left(\alpha_i\beta_i\right)^2 - 2d\left(\alpha_i^2 + \beta_i^2\right)\left(\alpha_i\beta_i\right)^2 - \left[1 + d\left(\alpha_i^2 + \beta_i^2\right)\right]\left(3\alpha_i^2 + 3\beta_i^2 + 4\alpha_i^2\beta_i^2 + \ldots\right) \\
&= 2\left(d-1\right)\left(\alpha_i\beta_i\right)^2 - \left[1 + d\left(\alpha_i^2 + \beta_i^2\right)\right]\left(3\alpha_i^2 + 3\beta_i^2 + 4\alpha_i^2\beta_i^2 + \ldots\right)
\end{aligned} \tag{30}$$

In equation (30), the higher-order terms that are not written explicitly (replaced by "...") contain only even powers of α_i and β_i, and thus are non-negative. In the last line of this equation, the quantity $2\left(d-1\right)\left(\alpha_i\beta_i\right)^2$ is negative for $d < 1$ and zero for $d = 1$ (or when either α_i or β_i is zero). Subtracted from this non-positive term is a sum of terms that are all non-negative because they contain only even powers of α_i and β_i. By this reasoning, every term in the difference $\eta_i^{\text{num}} - \eta_i^{\text{den}}$ either cancels or is non-positive. The numerator and denominator functions are equal only for the special case of $\alpha_i = \beta_i = 0$. Therefore, $\eta_i \leq 1$, with equality holding only in the special case where the LOS measurement is aligned with the boresight direction. Figure 1 plots the value of $\eta_i\left(\alpha_i, \beta_i, d\right)$ over a range of values of α_i and β_i for $d = 1$.

Note that one could also prove the upper and lower bounds on η_i by examining the matrices R_i^{FOCAL} and $\mathbb{R}_i^{\text{FOCAL}}$. As both matrices (and their inverses) are positive definite, the determinant of $R_i^{\text{FOCAL}}\left(\mathbb{R}_i^{\text{FOCAL}}\right)^{-1}$ will be strictly greater than zero. Next, Ref. [11] demonstrates that $\mathbb{R}_i^{\text{FOCAL}} \geq R_i^{\text{FOCAL}}$ in a positive-semidefinite sense. Consequently, the determinant of $\mathbb{R}_i^{\text{FOCAL}}$ is greater than or equal to the determinant of R_i^{FOCAL}. Division of the lesser determinant by the greater determinant will therefore always result in a value less than or equal to one, with equality holding only when the measurement is aligned with the boresight axis and the two matrices are equal.

Next, one can investigate the measurement covariance matrices R_i^{wFOV} and R_i^{QUEST} from the perspective of eigenvalues and eigenvectors. As discussed in Ref. [11], R_i^{QUEST} and R_i^{wFOV} have the same three eigenvectors. One of

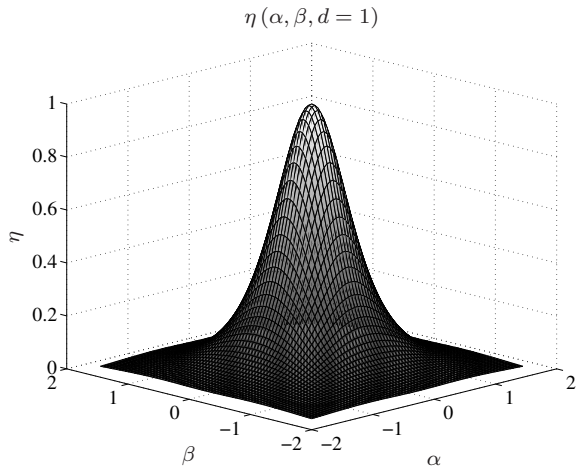

Figure 1. Scalar Function $\eta_i(\alpha_i, \beta_i, d)$ for $d = 1$.

these eigenvectors is the LOS measurement vector $\mathbf{b}_i$, with corresponds to an eigenvalue of zero. Furthermore, it can be easily verified that the remaining two eigenvalues of R_i^{QUEST} are both σ^2, independent of the specific measurement.

The two non-zero eigenvalues of the 3×3 matrix R_i^{wFOV}, λ_{wi}^+ and λ_{wi}^-, can be shown to be identical to the eigenvalues of the 2×2 matrix

$$\sigma^2 R_i^{\mathrm{FOCAL}} \left(\mathbb{R}_i^{\mathrm{FOCAL}}\right)^{-1} \tag{31}$$

The matrix product in equation (31) should be familiar from the definition of the function η_i. Because the characteristic function of a 2×2 matrix is quadratic, the eigenvalues of the matrix in equation (31) can be calculated analytically:

$$\begin{aligned}
\lambda_{wi}^+, \lambda_{wi}^- = & \frac{\sigma^2}{\left(1 + d\left(\alpha_i^2 + \beta_i^2\right)\right)\left(1 + \alpha_i^2 + \beta_i^2\right)^2} \\
& \times \left\{ \frac{1}{2}\left[\left(1 + d\alpha_i^2\right)^2\left(1 + \beta_i^2\right) + \left(1 + d\beta_i^2\right)^2\left(1 + \alpha_i^2\right) - 2\left(d\alpha_i\beta_i\right)^2\left(\alpha_i\beta_i\right)\right] \right. \\
& \pm \left. \sqrt{\begin{array}{l} \frac{1}{4}\left[\left(1 + d\alpha_i^2\right)^2\left(1 + \beta_i^2\right) - \left(1 + d\beta_i^2\right)^2\left(1 + \alpha_i^2\right)\right]^2 \\ + \left[\left(d\alpha_i\beta_i\right)^2\left(1 + \alpha_i^2\right) - \left(1 + d\alpha_i^2\right)^2\left(\alpha_i\beta_i\right)\right]\left[\left(d\alpha_i\beta_i\right)^2\left(1 + \beta_i^2\right) - \left(1 + d\beta_i^2\right)^2\left(\alpha_i\beta_i\right)\right] \end{array}} \right\}
\end{aligned} \tag{32}$$

Unfortunately, this expression is too complicated to provide much insight about eigenvalue magnitudes. Upper and lower bounds on the eigenvalues will be derived in a later section.

To show that the non-zero eigenvalues of R_i^{wFOV} are equal to those of equation (31), one must revisit the Jacobian

matrix J_i. As reported in Ref. [18], equation (9) can also be written in the form

$$J_i = \frac{1}{\left(1+\alpha_i^2+\beta_i^2\right)^{1/2}}\left\{-I_{3\times 3}+\mathbf{b}_i\mathbf{b}_i^{\mathrm{T}}\right\}\begin{bmatrix}1 & 0\\ 0 & 1\\ 0 & 0\end{bmatrix} = \frac{1}{\left(1+\alpha_i^2+\beta_i^2\right)^{1/2}}\left\{-I_{3\times 3}+\mathbf{b}_i\mathbf{b}_i^{\mathrm{T}}\right\} I_{3\times 2} \tag{33}$$

Within this equation, the matrix $\left\{-I_{3\times 3}+\mathbf{b}_i\mathbf{b}_i^{\mathrm{T}}\right\}$ is a scalar multiple of the matrix R_i^{QUEST}. After making the replacement,

$$J_i = -\frac{1}{\sigma^2\left(1+\alpha_i^2+\beta_i^2\right)^{1/2}} R_i^{\mathrm{QUEST}} I_{3\times 2} = -\frac{1}{\sigma^2\left(1+\alpha_i^2+\beta_i^2\right)^{1/2}} J_i \mathbb{R}_i^{\mathrm{FOCAL}} J_i^{\mathrm{T}} I_{3\times 2} \tag{34}$$

The 3×2 Jacobian J_i appears on both sides of equation (34): J_i is equal to a copy of itself times a 2×2 matrix expression. As J_i has rank 2, equation (34) implies the following:

$$-\frac{1}{\sigma^2\left(1+\alpha_i^2+\beta_i^2\right)^{1/2}} \mathbb{R}_i^{\mathrm{FOCAL}} J_i^{\mathrm{T}} I_{3\times 2} = I_{2\times 2} \tag{35}$$

or

$$\left(\mathbb{R}_i^{\mathrm{FOCAL}}\right)^{-1} = -\frac{1}{\sigma^2\left(1+\alpha_i^2+\beta_i^2\right)^{1/2}} J_i^{\mathrm{T}} I_{3\times 2} \tag{36}$$

Next, construct a new equation for R_i^{wFOV} by replacing the first Jacobian in equation (10) with the middle expression from equation (34):

$$R_i^{\mathrm{wFOV}} = -\frac{1}{\sigma^2\left(1+\alpha_i^2+\beta_i^2\right)^{1/2}} R_i^{\mathrm{QUEST}} I_{3\times 2} R_i^{\mathrm{FOCAL}} J_i^{\mathrm{T}} \tag{37}$$

Now post-multiply both sides of equation (37) by the rectangular matrix $I_{3\times 2}$, and substitute in equation (36):

$$\begin{aligned} R_i^{\mathrm{wFOV}} I_{3\times 2} &= -\frac{1}{\sigma^2\left(1+\alpha_i^2+\beta_i^2\right)^{1/2}} R_i^{\mathrm{QUEST}} I_{3\times 2} R_i^{\mathrm{FOCAL}} J_i^{\mathrm{T}} I_{3\times 2} \\ &= \frac{1}{\sigma^2} R_i^{\mathrm{QUEST}} I_{3\times 2} \sigma^2 R_i^{\mathrm{FOCAL}} \left(\mathbb{R}_i^{\mathrm{FOCAL}}\right)^{-1} \end{aligned} \tag{38}$$

Let $\mathbf{w}$ be a 3×1 eigenvector of R_i^{wFOV} corresponding to one of its non-zero eigenvalues λ_{wi}. Recall that $\mathbf{w}$ is also an eigenvector of R_i^{QUEST} with eigenvalue σ^2. Let $\mathbf{v}$ be a 2×1 eigenvector of the matrix $\sigma^2 R_i^{\mathrm{FOCAL}}\left(\mathbb{R}_i^{\mathrm{FOCAL}}\right)^{-1}$

corresponding to eigenvalue λ_{vi}. Pre-multiply the matrix in equation (38) by $\mathbf{w}^{\mathrm{T}}$, post-multiply by $\mathbf{v}$, and simplify:

$$\begin{aligned}\mathbf{w}^{\mathrm{T}} R_i^{\mathrm{wFOV}} I_{3\times 2}\mathbf{v} &= \lambda_{wi}\mathbf{w}^{\mathrm{T}}\begin{bmatrix}\mathbf{v}\\0\end{bmatrix}\\ &= \frac{1}{\sigma^2}\mathbf{w}^{\mathrm{T}} R_i^{\mathrm{QUEST}} I_{3\times 2}\sigma^2 R_i^{\mathrm{FOCAL}}\left(\mathbb{R}_i^{\mathrm{FOCAL}}\right)^{-1}\mathbf{v}\\ &= \frac{1}{\sigma^2}\sigma^2\mathbf{w}^{\mathrm{T}} I_{3\times 2}\mathbf{v}\lambda_{vi}\\ &= \mathbf{w}^{\mathrm{T}}\begin{bmatrix}\mathbf{v}\\0\end{bmatrix}\lambda_{vi}\end{aligned} \tag{39}$$

Comparison of the first and last lines of equation (39) presents two possibilities: either $\lambda_{wi} = \lambda_{vi}$, or $\mathbf{w}$ and $\begin{bmatrix}\mathbf{v}^{\mathrm{T}} & 0\end{bmatrix}^{\mathrm{T}}$ are orthogonal. Actually, both situations apply depending on which of the two possible $\mathbf{w}$ eigenvectors and which of the two possible $\mathbf{v}$ eigenvectors are selected. For a given eigenvector of R_i^{wFOV} and eigenvector of $\sigma^2 R_i^{\mathrm{FOCAL}}\left(\mathbb{R}_i^{\mathrm{FOCAL}}\right)^{-1}$, the eigenvalues will either match or the first two elements of $\mathbf{w}$ will be orthogonal to $\mathbf{v}$.

As the determinant of a matrix is the product of its eigenvalues, the product of the non-zero eigenvalues of R_i^{wFOV} is the determinant of the matrix $\sigma^2 R_i^{\mathrm{FOCAL}}\left(\mathbb{R}_i^{\mathrm{FOCAL}}\right)^{-1}$. Comparison with the implicit definition of η_i in equation (28) yields the expression

$$\lambda_{wi}^{+}\lambda_{wi}^{-} = \sigma^4\eta_i \tag{40}$$

At this point, all the necessary tools have been developed to compare the wide-FOV measurement model to the Cramér-Rao lower bound given by equation (23). To apply the wide-FOV measurement model in the context of a Kalman filter, one must find a way to handle the singularity of the covariance matrix R_i^{wFOV}. One such method, as applied to the EKF in Ref. [11], is to artificially add a rank-one update to the covariance matrix so that it can be inverted in the filter. This strategy closely resembles one typical approach to filtering using the QUEST measurement model. The rank-one update for the wide-FOV model takes the form

$$\mathcal{R}_i^{\mathrm{wFOV}} = R_i^{\mathrm{wFOV}} + \frac{1}{2}\mathrm{tr}\left(R_i^{\mathrm{wFOV}}\right)\mathbf{b}_i\mathbf{b}_i^{\mathrm{T}} \tag{41}$$

where the scalar coefficient of the update has been arbitrarily chosen to achieve good numerical properties.

Within the EKF, the attitude dynamics are linearized around the current best estimate of attitude. The linearized attitude part of the state vector is just the three-axis vector of small-angle attitude errors, $\boldsymbol{\delta}\mathbf{a}$. The linearized filter measurement equation relates the difference between the measured and estimated LOS unit vectors to the attitude error:

$$\Delta\mathbf{b}_i = \tilde{\mathbf{b}}_i - \hat{\mathbf{b}}_i = H_{bi}\boldsymbol{\delta}\mathbf{a} = [\mathbf{b}_i\times]\,\boldsymbol{\delta}\mathbf{a} \tag{42}$$

Note that in the actual filter, the H_{bi} measurement sensitivity matrix also contains columns corresponding to gyro

bias states and any other estimated states. Another caveat is that the matrix H_{bi} must be evaluated at the current best estimate of the vector $\mathbf{b}_i$, as the true vector is never available to the filter. This theoretical treatment focuses on the properties of the attitude part of the problem, and assumes that the estimates are sufficiently close to the true values for the necessary linearizations to be valid.

The EKF covariance update, written in information form, is given in equation (33) of Ref. [11] as

$$\left(P^{+}\right)^{-1} = \left(P^{-1}\right)^{-1} + H_{bi}^{\mathrm{T}}\left(\mathcal{R}_i^{\mathrm{wFOV}}\right)^{-1} H_{bi} \tag{43}$$

The inverses of the covariance matrices P^{-1} and P^{+}, which appear in equation (43), are known as information matrices. As this equation shows, the new information provided to the EKF by each measurement is given by the expression $H_{bi}^{\mathrm{T}}\left(\mathcal{R}_i^{\mathrm{wFOV}}\right)^{-1} H_{bi}$, where the updated (invertible) measurement covariance $\mathcal{R}_i^{\mathrm{wFOV}}$ has been used. This matrix expression can be compared to the single-measurement Fisher information matrix (FIM) derived in the previous section. For multiple LOS measurements at a given time, the update to the information matrix will just be a sum over the measurement index i of matrices of the form $H_{bi}^{\mathrm{T}}\left(\mathcal{R}_i^{\mathrm{wFOV}}\right)^{-1} H_{bi}$. The inverse of this sum can be compared to the Cramér-Rao lower bound (CRLB). It is possible to compare these quantities analytically, as follows.

One can use eigenvalue/eigenvector decomposition to write the wide-FOV measurement covariance matrix as:

$$R_i^{\mathrm{wFOV}} = \lambda_{wi}^{+}\mathbf{w}_{i+}\mathbf{w}_{i+}^{\mathrm{T}} + \lambda_{wi}^{-}\mathbf{w}_{i-}\mathbf{w}_{i-}^{\mathrm{T}} + (0)\,\mathbf{b}_i\mathbf{b}_i^{\mathrm{T}} \tag{44}$$

where λ_{wi}^{+} and λ_{wi}^{-} are the two non-zero eigenvalues of R_i^{wFOV}, with corresponding eigenvectors $\mathbf{w}_{i+}$ and $\mathbf{w}_{i-}$. The unit-length eigenvectors $\mathbf{w}_{i+}$, $\mathbf{w}_{i-}$, and $\mathbf{b}_i$ form an orthonormal triad such that $\mathbf{w}_{i+} \times \mathbf{w}_{i-} = \mathbf{b}_i$, $\mathbf{w}_{i-} \times \mathbf{b}_i = \mathbf{w}_{i+}$, and $\mathbf{b}_i \times \mathbf{w}_{i+} = \mathbf{w}_{i-}$. The new measurement covariance with the rank-one update has the same eigenvectors but no zero-valued eigenvalues. It can be decomposed as:

$$\mathcal{R}_i^{\mathrm{wFOV}} = \lambda_{wi}^{+}\mathbf{w}_{i+}\mathbf{w}_{i+}^{\mathrm{T}} + \lambda_{wi}^{-}\mathbf{w}_{i-}\mathbf{w}_{i-}^{\mathrm{T}} + \frac{\left(\lambda_{wi}^{+} + \lambda_{wi}^{-}\right)}{2}\mathbf{b}_i\mathbf{b}_i^{\mathrm{T}} \tag{45}$$

Equation (45) makes it simple to compute the inverse of $\mathcal{R}_i^{\mathrm{wFOV}}$:

$$\left(\mathcal{R}_i^{\mathrm{wFOV}}\right)^{-1} = \frac{1}{\lambda_{wi}^{+}}\mathbf{w}_{i+}\mathbf{w}_{i+}^{\mathrm{T}} + \frac{1}{\lambda_{wi}^{-}}\mathbf{w}_{i-}\mathbf{w}_{i-}^{\mathrm{T}} + \frac{2}{\left(\lambda_{wi}^{+} + \lambda_{wi}^{-}\right)}\mathbf{b}_i\mathbf{b}_i^{\mathrm{T}} \tag{46}$$

This expression for the matrix inverse can be used to compute the single-measurement update to the EKF information matrix:

$$H_{bi}^{\mathrm{T}}\left(\mathcal{R}_i^{\mathrm{wFOV}}\right)^{-1} H_{bi} = [\mathbf{b}_i\times]^{\mathrm{T}}\left\{\frac{1}{\lambda_{wi}^{+}}\mathbf{w}_{i+}\mathbf{w}_{i+}^{\mathrm{T}} + \frac{1}{\lambda_{wi}^{-}}\mathbf{w}_{i-}\mathbf{w}_{i-}^{\mathrm{T}} + \frac{2}{\left(\lambda_{wi}^{+} + \lambda_{wi}^{-}\right)}\mathbf{b}_i\mathbf{b}_i^{\mathrm{T}}\right\}[\mathbf{b}_i\times] \tag{47}$$

By employing the cross product relationships of the orthonormal triad of eigenvectors, equation (47) can be simplified to obtain:

$$H_{bi}^{\mathrm{T}}\left(\mathcal{R}_i^{\mathrm{wFOV}}\right)^{-1} H_{bi} = \frac{1}{\lambda_{wi}^{-}}\mathbf{w}_{i+}\mathbf{w}_{i+}^{\mathrm{T}} + \frac{1}{\lambda_{wi}^{+}}\mathbf{w}_{i-}\mathbf{w}_{i-}^{\mathrm{T}} + (0)\,\mathbf{b}_i\mathbf{b}_i^{\mathrm{T}} \tag{48}$$

Note how the rank-one update that made $\mathcal{R}_i^{\mathrm{wFOV}}$ invertible does not affect the amount of information available to the filter in equation (48).

Now compare equation (48) to $H_i^{\mathrm{T}}\left(R_i^{\mathrm{FOCAL}}\right)^{-1} H_i$, the derived single-measurement FIM based on linearization around the two-dimensional sensor measurements. From equation (28), the FIM can be written as

$$H_i^{\mathrm{T}}\left(R_i^{\mathrm{FOCAL}}\right)^{-1} H_i = \frac{1}{\sigma^4\eta_i} R_i^{\mathrm{wFOV}} \tag{49}$$

Substitution of the eigenvalue/eigenvector decomposition of equation (44) into equation (49) yields

$$H_i^{\mathrm{T}}\left(R_i^{\mathrm{FOCAL}}\right)^{-1} H_i = \frac{\lambda_{wi}^{+}}{\sigma^4\eta_i}\mathbf{w}_{i+}\mathbf{w}_{i+}^{\mathrm{T}} + \frac{\lambda_{wi}^{-}}{\sigma^4\eta_i}\mathbf{w}_{i-}\mathbf{w}_{i-}^{\mathrm{T}} \tag{50}$$

The one-measurement increment to the EKF information matrix, $H_{bi}^{\mathrm{T}}\left(\mathcal{R}_i^{\mathrm{wFOV}}\right)^{-1} H_{bi}$, should not exceed the theoretical upper bound of the one-measurement Fisher information matrix in a positive-semidefinite sense. One can compare the two matrices by subtracting equation (48) from equation (50):

$$H_i^{\mathrm{T}}\left(R_i^{\mathrm{FOCAL}}\right)^{-1} H_i - H_{bi}^{\mathrm{T}}\left(\mathcal{R}_i^{\mathrm{wFOV}}\right)^{-1} H_{bi} = \frac{\lambda_{wi}^{+}\lambda_{wi}^{-} - \sigma^4\eta_i}{\sigma^4\eta_i\lambda_{wi}^{-}}\mathbf{w}_{i+}\mathbf{w}_{i+}^{\mathrm{T}} + \frac{\lambda_{wi}^{+}\lambda_{wi}^{-} - \sigma^4\eta_i}{\sigma^4\eta_i\lambda_{wi}^{+}}\mathbf{w}_{i-}\mathbf{w}_{i-}^{\mathrm{T}} \tag{51}$$

From equation (40), however, $\lambda_{wi}^{+}\lambda_{wi}^{-} = \sigma^4\eta_i$, so the two matrices are analytically identical. This result implies that the wide-FOV measurement model achieves the Cramér-Rao lower bound. The appropriate covariance definition for the wide-FOV model is defined in a manner analogous to equation (23):

$$P^{\mathrm{wFOV}} = \left[\sum_{i=1}^{N} H_{bi}^{\mathrm{T}}\left(\mathcal{R}_i^{\mathrm{wFOV}}\right)^{-1} H_{bi}\right]^{-1} = \sigma^4\left[\sum_{i=1}^{N}\eta_i^{-1}R_i^{\mathrm{wFOV}}\right]^{-1} = P^{\mathrm{DIRECT}} \tag{52}$$

QUEST AND THE CRAMÉR-RAO LOWER BOUND

Now compare the matrices P^{QUEST} and $P^{\mathrm{wFOV}} = P^{\mathrm{DIRECT}}$, repeated here:

$$P^{\mathrm{QUEST}} = \sigma^4\left[\sum_{i=1}^{N} R_i^{\mathrm{QUEST}}\right]^{-1} = \sigma^4\left[\sum_{i=1}^{N} J_i\mathbb{R}_i^{\mathrm{FOCAL}}J_i^{\mathrm{T}}\right]^{-1} \tag{53a}$$

$$P^{\mathrm{wFOV}} = P^{\mathrm{DIRECT}} = \sigma^4\left[\sum_{i=1}^{N}\eta_i^{-1}R_i^{\mathrm{wFOV}}\right]^{-1} = \sigma^4\left[\sum_{i=1}^{N} J_i\eta_i^{-1}R_i^{\mathrm{FOCAL}}J_i^{\mathrm{T}}\right]^{-1} \tag{53b}$$

The previous section shows that $P^{\mathrm{wFOV}} = P^{\mathrm{DIRECT}}$, and Ref. [11] demonstrates that $R_i^{\mathrm{wFOV}} \leq R_i^{\mathrm{QUEST}}$. It is now possible to show that $P^{\mathrm{QUEST}} \geq P^{\mathrm{wFOV}}$. The following statements are all equivalent:

$$P^{\mathrm{QUEST}} \geq P^{\mathrm{wFOV}} \tag{54a}$$

$$P^{\mathrm{QUEST}} - P^{\mathrm{wFOV}} \geq 0 \tag{54b}$$

$$\left(P^{\mathrm{wFOV}}\right)^{-1} - \left(P^{\mathrm{QUEST}}\right)^{-1} \geq 0 \tag{54c}$$

$$\sum_{i=1}^{N} \eta_i^{-1} R_i^{\mathrm{wFOV}} - \sum_{i=1}^{N} R_i^{\mathrm{QUEST}} \geq 0 \tag{54d}$$

$$\sum_{i=1}^{N} J_i \eta_i^{-1} R_i^{\mathrm{FOCAL}} J_i^{\mathrm{T}} - \sum_{i=1}^{N} J_i \mathbb{R}_i^{\mathrm{FOCAL}} J_i^{\mathrm{T}} \geq 0 \tag{54e}$$

One way to show equation (54e) is to show that the inequality holds term-by-term for every term, such that

$$J_i \eta_i^{-1} R_i^{\mathrm{FOCAL}} J_i^{\mathrm{T}} - J_i \mathbb{R}_i^{\mathrm{FOCAL}} J_i^{\mathrm{T}} = J_i \left(\eta_i^{-1} R_i^{\mathrm{FOCAL}} - \mathbb{R}_i^{\mathrm{FOCAL}}\right) J_i^{\mathrm{T}} \geq 0 \qquad \forall i \in (1, 2, \ldots, N) \tag{55}$$

or just

$$\eta_i^{-1} R_i^{\mathrm{FOCAL}} - \mathbb{R}_i^{\mathrm{FOCAL}} \geq 0 \qquad \forall i \in (1, 2, \ldots, N) \tag{56}$$

The following proof shows that equation (56) holds for all α_i, β_i, and $0 \leq d \leq 1$. Another way to write equation (56) is

$$R_i^{\mathrm{FOCAL}} - \eta_i \mathbb{R}_i^{\mathrm{FOCAL}} \geq 0 \tag{57}$$

The eigenvalues of $\eta_i \mathbb{R}_i^{\mathrm{FOCAL}}$ are $\eta_i \sigma^2 \left(1 + \alpha_i^2 + \beta_i^2\right)$ and $\eta_i \sigma^2 \left(1 + \alpha_i^2 + \beta_i^2\right)^2$. Therefore, $\eta_i \mathbb{R}_i^{\mathrm{FOCAL}} \leq \eta_i \sigma^2 \left(1 + \alpha_i^2 + \beta_i^2\right)^2 I_{2\times 2}$. As a result,

$$R_i^{\mathrm{FOCAL}} - \eta_i \mathbb{R}_i^{\mathrm{FOCAL}} \geq R_i^{\mathrm{FOCAL}} - \eta_i \sigma^2 \left(1 + \alpha_i^2 + \beta_i^2\right)^2 I_{2\times 2} \tag{58}$$

If the right-hand quantity in equation (58) is positive-semidefinite, than so is the quantity of interest on the left-hand side. Writing everything in terms of α_i and β_i gives

$$\begin{aligned} &R_i^{\mathrm{FOCAL}} - \eta_i \sigma^2 \left(1 + \alpha_i^2 + \beta_i^2\right)^2 I_{2\times 2} \\ &\quad = \frac{\sigma^2}{1 + d\left(\alpha_i^2 + \beta_i^2\right)} \begin{bmatrix} \left(1 + d\alpha_i^2\right)^2 & \left(d\alpha_i\beta_i\right)^2 \\ \left(d\alpha_i\beta_i\right)^2 & \left(1 + d\beta_i^2\right)^2 \end{bmatrix} - \frac{\sigma^2 \left[\left(1 + d\alpha_i^2\right)\left(1 + d\beta_i^2\right) + \left(d\alpha_i\beta_i\right)^2\right]}{\left(1 + \alpha_i^2 + \beta_i^2\right)\left(1 + d\left(\alpha_i^2 + \beta_i^2\right)\right)} \begin{bmatrix} 1 & 0 \\ 0 & 1 \end{bmatrix} \end{aligned} \tag{59}$$

After significant algebra, equation (59) reduces to

$$R_i^{\mathrm{FOCAL}} - \eta_i\sigma^2\left(1+\alpha_i^2+\beta_i^2\right)^2 I_{2\times 2} = \frac{\sigma^2(1-d)\left(\alpha_i^2+\beta_i^2+2d\alpha_i^2\beta_i^2\right)}{\left(1+\alpha_i^2+\beta_i^2\right)\left(1+d\left(\alpha_i^2+\beta_i^2\right)\right)}\begin{bmatrix}1 & 0\\ 0 & 1\end{bmatrix} + \frac{2\sigma^2 d}{\left(1+\alpha_i^2+\beta_i^2\right)\left(1+d\left(\alpha_i^2+\beta_i^2\right)\right)}\begin{bmatrix}\alpha_i^2\left(1+\alpha_i^2\right) & 0\\ 0 & \beta_i^2\left(1+\beta_i^2\right)\end{bmatrix} + \frac{\sigma^2 d^2}{1+d\left(\alpha_i^2+\beta_i^2\right)}\begin{bmatrix}\alpha_i^4 & \left(\alpha_i\beta_i\right)^2\\ \left(\alpha_i\beta_i\right)^2 & \beta_i^4\end{bmatrix} \tag{60}$$

In this equation, the matrix difference on the left-hand side is equal to the sum of three matrices on the right-hand side. The first of these three matrices is just a non-negative scalar times the identity matrix. The scalar goes to zero only when $d = 1$ or when $\alpha_i = \beta_i = 0$; for all other values (provided $0 \leq d \leq 1$) it is positive. Therefore this first matrix is positive-semidefinite. The second matrix is also positive-semidefinite, because it is the product of a different non-negative scalar and a diagonal matrix with non-negative diagonal entries. The third matrix on the right-hand side of equation (60) is not diagonal, but it too is positive-semidefinite. One can easily calculate that it has the non-negative eigenvalues 0 and $\sigma^2 d^2\left(\alpha_i^4+\beta_i^4\right)/\left(1+d\left(\alpha_i^2+\beta_i^2\right)\right)$. As the quantity of interest can be written as a sum of three positive-semidefinite matrices, it must be positive-semidefinite itself. Furthermore, the three matrices never go to zero simultaneously except when $\alpha_i = \beta_i = 0$. Therefore $R_i^{\mathrm{FOCAL}} \geq \eta_i \mathbb{R}_i^{\mathrm{FOCAL}}$, and by consequence, $P^{\mathrm{QUEST}} \geq P^{\mathrm{wFOV}} = P^{\mathrm{DIRECT}}$. This result implies, as expected, that the filter based on the QUEST measurement model is bounded away from the CRLB except in the case where the measurement is aligned with the boresight and $\alpha_i = \beta_i = 0$.

FURTHER COVARIANCE PROPERTIES

The previous sections derived some matrix inequalities to compare the measurement covariance matrices R_i^{wFOV} and R_i^{QUEST} and the attitude error covariance matrices P^{wFOV} and P^{QUEST}. This section uses some of these previous results to examine the eigenvalues of these matrices. While equation (32) gives an exact analytical expression for the non-zero eigenvalues of R_i^{wFOV}, this expression is too complicated to provide much insight about eigenvalue magnitudes. An alternative approach seeks bounds on the eigenvalue magnitudes based on the previously derived matrix inequalities.

Reference [11] demonstrates that $R_i^{\mathrm{QUEST}} \geq R_i^{\mathrm{wFOV}}$. As a logical consequence of equation (57), in combination with the expressions for R_i^{wFOV} and R_i^{QUEST} in Eqs. (10) and (11), one can infer that $\eta_i^{-1} R_i^{\mathrm{wFOV}} \geq R_i^{\mathrm{QUEST}}$.

Combination of these two matrix inequalities yields:

$$\eta_i^{-1} R_i^{\mathrm{wFOV}} \geq R_i^{\mathrm{QUEST}} \geq R_i^{\mathrm{wFOV}} \tag{61}$$

Suppose that the vector $\mathbf{v}$ is a unit-length eigenvector of R_i^{wFOV} corresponding to either of its non-zero eigenvalues, and recall that the quadratic expression $\mathbf{v}^{\mathrm{T}} R_i^{\mathrm{wFOV}} \mathbf{v}$ yields that eigenvalue. The vector $\mathbf{v}$ is also an eigenvector of R_i^{QUEST} corresponding to one of its σ^2 eigenvalues. By the definition of the matrix inequality, equation (61) implies

$$\eta_i^{-1} \mathbf{v}^{\mathrm{T}} R_i^{\mathrm{wFOV}} \mathbf{v} \geq \mathbf{v}^{\mathrm{T}} R_i^{\mathrm{QUEST}} \mathbf{v} \geq \mathbf{v}^{\mathrm{T}} R_i^{\mathrm{wFOV}} \mathbf{v} \tag{62}$$

which can be simplified as

$$\eta_i^{-1} \lambda_{wi} \geq \sigma^2 \geq \lambda_{wi} \tag{63}$$

Note that the leftmost term of the inequality is equivalent to the corresponding eigenvalue of $\eta_i^{-1} R_i^{\mathrm{wFOV}}$.

The first two terms of equation (63) yield $\lambda_{wi} \geq \eta_i \sigma^2$, and the last two terms yield $\lambda_{wi} \leq \sigma^2$. Putting these inequalities together, the non-zero eigenvalues of R_i^{wFOV} are bounded according to

$$\eta_i \sigma^2 \leq \lambda_{wi} \leq \sigma^2 \tag{64}$$

Bounds can also be found for the eigenvalues of $\eta_i^{-1} R_i^{\mathrm{wFOV}}$, a matrix that is closely related to the one-measurement FIM as described in equation (49). These are given by $\lambda_{di} = \eta_i^{-1} \lambda_{wi}$. Multiplication of equation (64) by η_i^{-1} gives

$$\sigma^2 \leq \lambda_{di} \leq \eta_i^{-1} \sigma^2 \tag{65}$$

The bounds on the non-zero eigenvalues of R_i^{QUEST}, R_i^{wFOV}, and $\eta_i^{-1} R_i^{\mathrm{wFOV}}$ can be used to determine lower bounds on the eigenvalues of P^{QUEST} and $P^{\mathrm{wFOV}} = P^{\mathrm{DIRECT}}$. Upper bounds cannot be found, as these matrices tend to infinity if the available LOS measurements are not sufficiently independent. In what follows, it is assumed that independent measurements are available, so that finite, invertible matrices P^{QUEST} and P^{wFOV} exist. The derivations also make use of the fact that the minimum eigenvalue of a positive definite matrix is the inverse of the maximum eigenvalue of the matrix inverse.

The inverses of P^{QUEST} and P^{wFOV} are found from equation (53):

$$\left(P^{\mathrm{QUEST}}\right)^{-1} = \frac{1}{\sigma^4} \left[\sum_{i=1}^{N} R_i^{\mathrm{QUEST}} \right] \tag{66a}$$

$$\left(P^{\mathrm{wFOV}}\right)^{-1} = \frac{1}{\sigma^4}\left[\sum_{i=1}^{N} \eta_i^{-1} R_i^{\mathrm{wFOV}}\right] \tag{66b}$$

Suppose that $\mathbf{v}$ is an eigenvector of $\left(P^{\mathrm{QUEST}}\right)^{-1}$. Then the corresponding eigenvalue is given by

$$\lambda_{Pq}^{-1} = \mathbf{v}^{\mathrm{T}}\left(P^{\mathrm{QUEST}}\right)^{-1}\mathbf{v} = \frac{1}{\sigma^4}\left(\mathbf{v}^{\mathrm{T}} R_1^{\mathrm{QUEST}}\mathbf{v} + \mathbf{v}^{\mathrm{T}} R_2^{\mathrm{QUEST}}\mathbf{v} + \ldots + \mathbf{v}^{\mathrm{T}} R_N^{\mathrm{QUEST}}\mathbf{v}\right) \tag{67}$$

Each term on the right-hand side is maximized when $\mathbf{v}$ is also an eigenvector of R_i^{QUEST} corresponding to its maximum eigenvalues of σ^2. An upper bound on λ_{Pq}^{-1} occurs in the limit as this holds for every term in the summation:

$$\lambda_{Pq}^{-1} \leq \frac{1}{\sigma^4}\left(\sigma^2 + \sigma^2 + \ldots + \sigma^2\right) = \frac{1}{\sigma^4} N\sigma^2 = \frac{N}{\sigma^2} \tag{68}$$

The corresponding lower bound on the eigenvalues of P^{QUEST} is then

$$\lambda_{Pq} \geq \frac{\sigma^2}{N} \tag{69}$$

The calculations are slightly more complicated for P^{wFOV}. Suppose that $\mathbf{v}$ is an eigenvector of $\left(P^{\mathrm{wFOV}}\right)^{-1}$, so that the corresponding eigenvalue is:

$$\lambda_{Pw}^{-1} = \mathbf{v}^{\mathrm{T}}\left(P^{\mathrm{DIRECT}}\right)^{-1}\mathbf{v} = \frac{1}{\sigma^4}\left(\mathbf{v}^{\mathrm{T}}\eta_1^{-1} R_1^{\mathrm{wFOV}}\mathbf{v} + \mathbf{v}^{\mathrm{T}}\eta_2^{-1} R_2^{\mathrm{wFOV}}\mathbf{v} + \ldots + \mathbf{v}^{\mathrm{T}}\eta_N^{-1} R_N^{\mathrm{wFOV}}\mathbf{v}\right) \tag{70}$$

The terms on the right-hand side are each bounded above by the maximum eigenvalue of any of the $\eta_i^{-1} R_i^{\mathrm{wFOV}}$ matrices, which is a measurement-dependent quantity. Each matrix $\eta_i^{-1} R_i^{\mathrm{wFOV}}$ individually has a maximum eigenvalue of $\eta_i^{-1}\sigma^2$, as specified in equation (65). The maximum over all measurements corresponds to $\eta_{\min}$, the minimum value of η_i for all $i = 1, 2, \ldots, N$. Therefore, λ_{Pw}^{-1} is bounded above by

$$\lambda_{Pw}^{-1} \leq \frac{1}{\sigma^4}\left(\eta_{\min}^{-1}\sigma^2 + \eta_{\min}^{-1}\sigma^2 + \ldots + \eta_{\min}^{-1}\sigma^2\right) = \frac{1}{\sigma^4}\eta_{\min}^{-1} N\sigma^2 = \eta_{\min}^{-1}\frac{N}{\sigma^2} \tag{71}$$

This upper bound on the eigenvalues of $\left(P^{\mathrm{wFOV}}\right)^{-1}$ corresponds to a lower bound on the eigenvalues of P^{wFOV}:

$$\lambda_{Pw} \geq \eta_{\min}\frac{\sigma^2}{N} \tag{72}$$

The lower bounds given by Eqs. (69) and (72) are closely related to the theoretical maximum information (in the sense of Fisher) available via the measurement models.

SIMULATIONS

The simulations of Ref. [11] have been repeated with the addition of an EKF that uses the two-dimensional sensor measurement model directly instead of converting the measurements to LOS unit vectors. This papers' theoretical results show that the wide-FOV measurement model achieves the CRLB, which was derived from the sensor measurement model. One would expect, therefore, that the wide-FOV model performance would be very similar to the performance of the 2-d sensor model in simulations.

The original simulations of Ref. [11] involve a spacecraft performing a docking-like maneuver with linear motion and rotation. A simulated VISNAV camera sensor provides LOS unit vector measurements to eight beacons, and gyro measurements are also available. The EKF states are 3-axis attitude errors and 3-axis gyro bias errors. For more simulation details, see Ref. [11].

Two different filter implementations for the wide-FOV model are described in Ref. [11]. One of them addresses the singularity of R_i^{wFOV} by performing a transformation based on an eigenvalue/eigenvector covariance decomposition. The other adds a rank-one update to R_i^{wFOV} to make the resulting matrix invertible. Both approaches give the same measurement updates, but Ref. [11] found that in practice the decomposition approach is more sensitive to numerical ill-conditioning. Consequently, this paper's analyses and simulations focus on the EKF with the rank-one covariance update.

As predicted, the EKFs based on the direct sensor model and the wide-FOV measurement model produce results that are nearly identical. Reference [11] found that the 3σ bounds for the QUEST and wide-FOV models differed by about 30%. In contrast, the wide-FOV and direct measurement models had an average difference of $2.6 \times 10^{-6}\%$ for the case with zero initial estimation error. When an initial estimation error of about 6° was chosen, consistent with the initial filter covariance assumptions, the average difference in the 3σ bounds was less than 0.01%.

Figures 2, 3, and 4 give the attitude estimation errors and 3σ bounds in the roll, pitch, and yaw axes, respectively. It

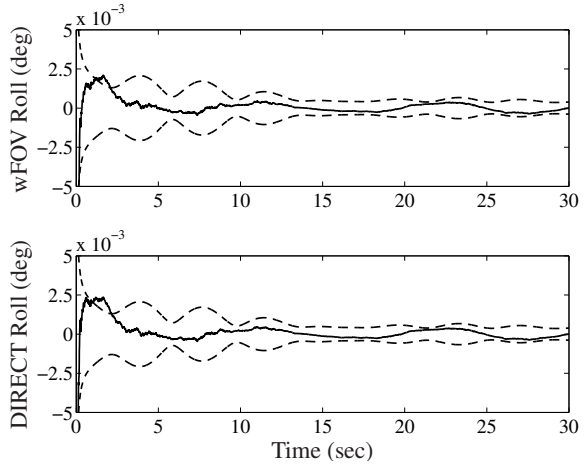

Figure 2. Roll-Axis Errors with 3σ Bounds

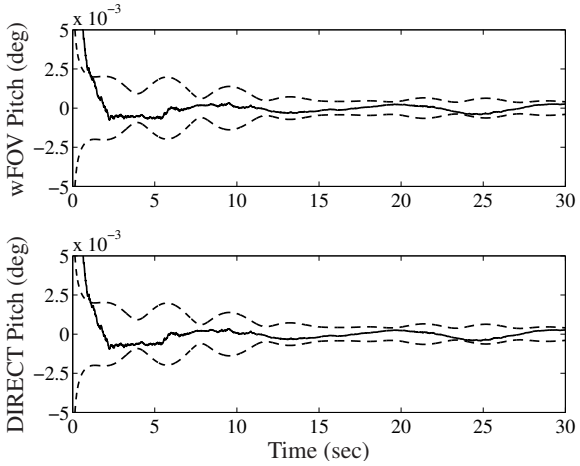

Figure 3. Pitch-Axis Errors with 3σ Bounds

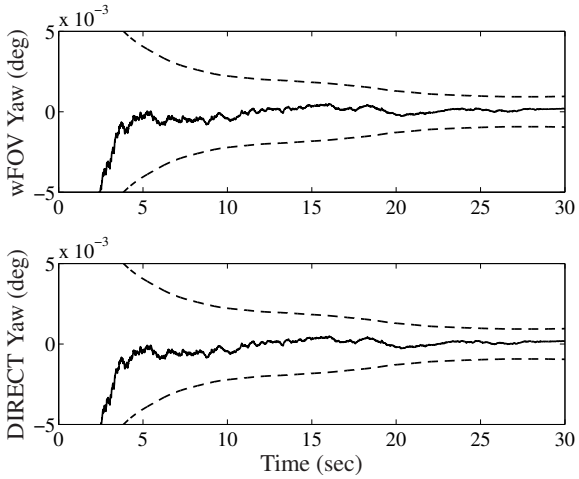

Figure 4. Yaw-Axis Errors with 3σ Bounds

is very hard to distinguish between the wide-FOV and DIRECT filters based on visual inspection of Figs. 2, 3, and 4. To make the comparison more clear, the differences and percent differences of various quantities are also plotted.

Figures 5 and 6 compare the standard deviations for the EKFs based on the QUEST measurement model and the DIRECT measurement model. The differences between the two models are nearly identical to the differences between the QUEST and wide-FOV models in Ref. [11].

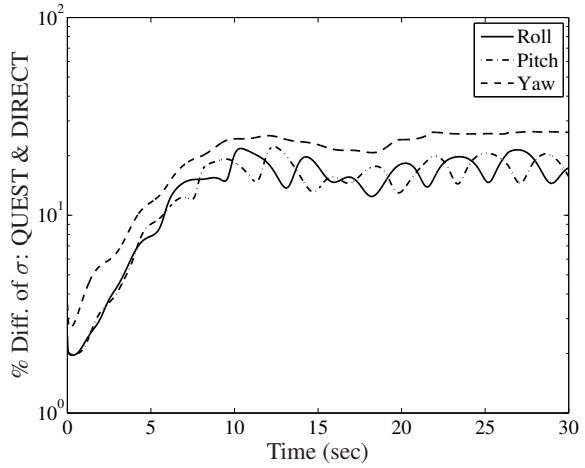

Figure 5. Percent Difference of Standard Deviation: QUEST and DIRECT

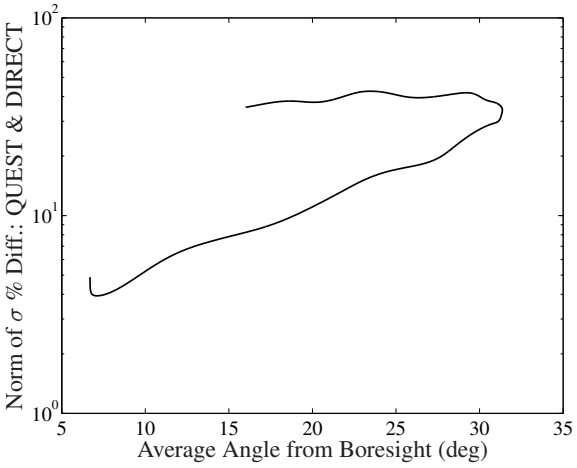

Figure 6. Norm of Percent Difference in σ: QUEST and DIRECT

Figures 7 and 8 show the standard deviation percent differences for the EKFs that employ the wide-FOV and DIRECT measurement models. These percent differences are orders of magnitude smaller than those of Figs. 5 and 6. Actually the standard deviations are identical from an analytical perspective, but there are small numerical differences.

Although the standard deviations of the wide-FOV and DIRECT models are essentially identical, Fig. 9 shows that

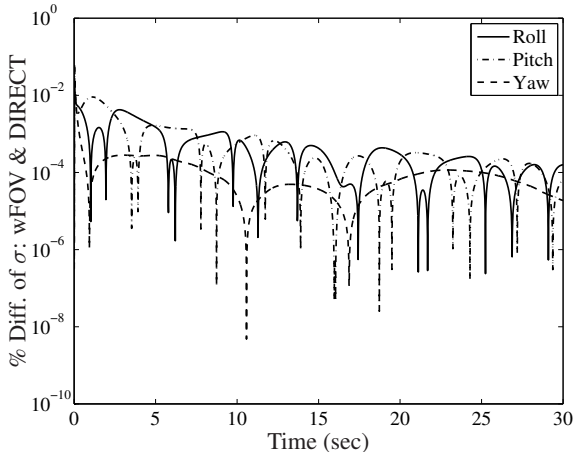

Figure 7. Percent Difference of Standard Deviation: wFOV and DIRECT

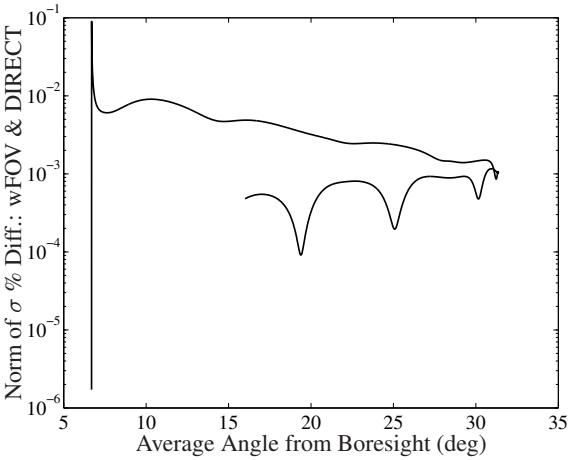

Figure 8. Norm of Percent Difference in σ: wFOV and DIRECT

there are small differences in the estimated attitude for the two measurement models. In contrast, the differences in attitude estimates between the QUEST and DIRECT methods are much larger, as illustrated in Fig. 10.

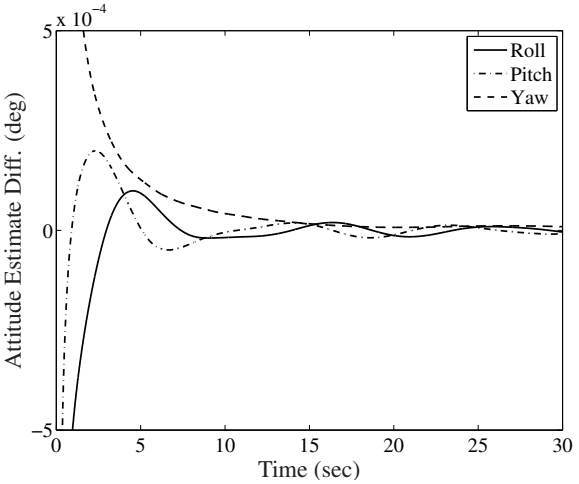

Figure 9. Difference of Attitude Estimates: wFOV and DIRECT

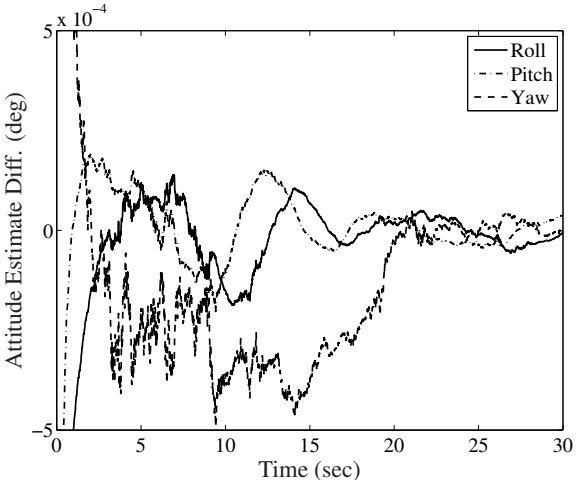

Figure 10. Difference of Attitude Estimates: QUEST and DIRECT

The normalized measurement innovation statistics (normalized innovation errors squared) for the QUEST, wide-FOV, and DIRECT measurement models are plotted in Fig. 11. The figure also shows the associated $99\%\chi^2$ bounds for this statistic. The bounds assume two-dimensional measurements, which is appropriate for three-dimensional LOS vectors that are constrained to have unit length. As evidenced in the figure, the wide-FOV and DIRECT models more closely agree with the theoretical bounds.

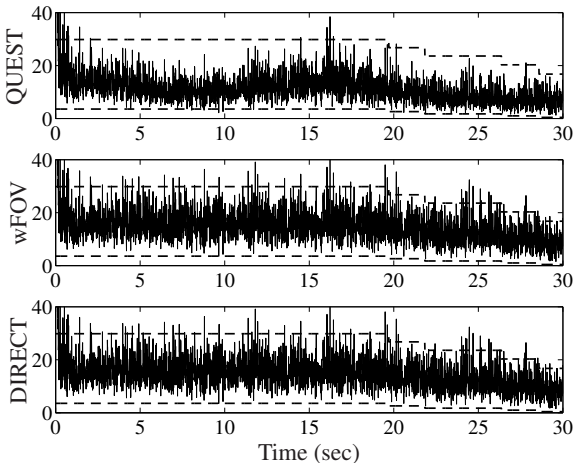

Figure 11. Normalized Measurement Innovation Statistics with χ^2 Bounds

CONCLUSIONS

This paper analyzed the new wide field-of-view (FOV) measurement model for attitude determination with unit vector measurements. The wide-FOV model accounts for the changing measurement error covariance far from the sensor boresight, rather than assuming all measurements are equally accurate. In contrast, the classic QUEST measurement model assumes that errors are uniformly distributed around the measurement direction. The wide-FOV and QUEST measurement models were compared to a scheme that uses the two-dimensional sensor focal plane measurements directly, without first converting them to unit vectors. The Fisher information matrix and Cramér-Rao lower bound for this direct model were derived, and the wide-FOV model was shown to achieve this bound. This result implies that no other unit-vector measurement model can outperform the wide-FOV model for the given sensor. Numerical simulations confirm these results by demonstrating that the 3σ bounds were effectively identical for filters based on the direct focal plane measurements and filters that use the wide-FOV model.

REFERENCES

[1] G. Wahba, "A Least Squares Estimate of Satellite Attitude," *SIAM Review*, Vol. 7, No. 3, 1965, p. 409.

[2] J. W. Murrell, "Precision Attitude Determination for Multimission Spacecraft," *AIAA Guidance, Navigation, and Control Conference*, Aug. 7-9, 1978, pp. 70–87.

[3] E. J. Lefferts, F. L. Markley, and M. D. Shuster, "Kalman Filtering for Spacecraft Attitude Estimation," *Journal of Guidance, Control, and Dynamics*, Vol. 5, No. 5, Sept.-Oct. 1982, pp. 417–429.

[4] M. D. Shuster, "A Simple Kalman Filter and Smoother for Spacecraft Attitude," *Journal of the Astronautical Sciences*, Vol. 37, No. 1, 1989, pp. 89–106.

[5] M. D. Shuster, "Kalman Filtering of Spacecraft Attitude and the QUEST Model," *Journal of the Astronautical Sciences*, Vol. 38, July-Sept. 1990, pp. 377–393.

[6] J. L. Crassidis, F. L. Markley, and Y. Cheng, "Survey of Nonlinear Attitude Estimation Methods," *Journal of Guidance, Control, and Dynamics*, Vol. 30, No. 1, Jan.-Feb. 2007, pp. 12–28.

[7] J. R. Wertz, *Mission Geometry; Orbit and Constellation Design and Management*. Microcosm Press, El Segundo, CA and Kluwer Academic Publishers, Dordrecht, Netherlands, 2001. Chapter 3, pp. 152–167.

[8] M. D. Shuster and S. D. Oh, "Three-Axis Attitude Determination from Vector Observations," *Journal of Guidance and Control*, Vol. 4, No. 1, Jan.-Feb. 1981, pp. 70–77.

[9] G. Ju and J. L. Junkins, "Overview of Star Tracker Technology and its Trends in Research and Development," *Advances in the Astronautical Sciences, The John L. Junkins Astrodynamics Symposium*, Vol. 115, 2003, pp. 461–478.

[10] J. L. Junkins, D. C. Hughes, K. P. Wazni, and V. Pariyapong, "Vision-Based Navigation for Rendezvous, Docking, and Proximity Operations," *22nd Annual AAS Guidance and Control Conf., Breckenridge, CO*, No. AAS-99-021, Feb. 7-10, 1999.

[11] Y. Cheng, J. L. Crassidis, and F. L. Markley, "Attitude Estimation for Large Field-of-View Sensors," *Journal of the Astronautical Sciences*, Vol. 54, July-Dec. 2006, pp. 433–448.

[12] M. D. Shuster, "Maximum Likelihood Estimation of Spacecraft Attitude," *Journal of the Astronautical Sciences*, Vol. 37, No. 1, 1989, pp. 79–88.

[13] M. D. Shuster, "Constraint in Attitude Estimation Part I: Constrained Estimation," *Journal of the Astronautical Sciences*, Vol. 51, No. 1, Jan.-March 2003, pp. 51–74.

[14] D. Mortari and M. Manoranjan, "Multiplicative Measurement Model," *Journal of the Astronautical Sciences*, Vol. 57, No. 1-2, Jan.-June 2009, pp. 47–60.

[15] D. L. Light, *Satellite Photogrammetry*, ch. Chapter 17. American Society of Photogrammetry, 4 ed., 1980.

[16] M. D. Shuster, "Erratum: Kalman Filtering of Spacecraft Attitude and the QUEST Model," *Journal of the Astronautical Sciences*, Vol. 51, July-Sept. 2003, p. 359.

[17] J. L. Crassidis and J. L. Junkins, *Optimal Estimation of Dynamic Systems*. Chapman & Hall/CRC, Boca Raton, FL, 2 ed., 2011. Chapter 2.

[18] R. Zanetti, "A Multiplicative Residual Approach to Attitude Kalman Filtering with Unit-Vector Measurements," *Journal of the Astronautical Sciences*, Vol. 57, No. 4, 2010, pp. 793–801.